Journal of Power and Energy Engineering, 2016, 4, 56-66
Published Online April 2016 in SciRes. http://www.scirp.org/journal/jpee
http://dx.doi.org/10.4236/jpee.2016.44006

Scientific Research Publishing

Assessment of Operating Condition Dependent Reliability Indices in Microgrids

Rafael Medeiros, Xufeng Xu, Elham Makram

Department of Electrical and Computer Engineering, Clemson University, Clemson, SC, USA
Email: rmedeir@clemson.edu, xufengx@g.clemson.edu, makram@clemson.edu

Received 27 March 2016; accepted 26 April 2016; published 29 April 2016

Abstract

Reliability results are important for proper planning and operation of utility companies. At the base of this method of analysis is the failure rate of the system components. In the traditional method, this probability of failure is determined by the components' manufacturer and is considered to be constant. This study proposes a dynamic modeling of failure rate, taking the system operating conditions into consideration. With this new consideration, an IEEE test system has seven of its reliability indices quantified for comparison. The inclusion of the newly modeled failure rate leads to a worsening of 11.07% in the indices, on average. A second analysis is performed considering the presence of DG sources within the microgrid, namely PV and wind based. An improvement of 0.71% on the indices is noticed, once the DG sources are introduced. Finally, the effects of storage systems in the microgrid are investigated through a third scenario, in which two 2 MWh battery systems are introduced, and an improvement of 3.05% is noticed in the reliability indices.

Keywords

Failure Rate, Microgrid, Power Flow, Reliability Assessment, Renewables, Storage

1. Introduction

It is expected of a reliable power system to be able to respond quickly and efficiently to faults, keeping customer disconnections to a minimum, both in quantities, as well as in duration. Billinton [1] presents the standard analysis for reliability of supply on a distribution system. This method consists of determining the probability of failure (failure rate) of every element in the system, and for each of these possible faults, analyzing what load points (LPs) have supply cut off, and for what duration.

How to cite this paper: Medeiros, R., Xu, X.F. and Makram, E. (2016) Assessment of Operating Condition Dependent Reliability Indices in Microgrids. *Journal of Power and Energy Engineering*, **4**, 56-66. http://dx.doi.org/10.4236/jpee.2016.44006

This traditional analysis has been applied to microgrids, regarding these systems as distributions systems with embedded microsources of generation. Bae *et al.* [2] propose a technique for reliability evaluation including characteristics of DG source operation, such as operation mode and possibility of malfunctioning of the source itself. This study is extended in [3], where grid customers are considered to contractually belong to different microgrids, where their respective micro sources will give priority of supply to customers within that one microgrid. The impacts of storage system, in addition to micro sources are investigated in [4], in terms of reliability and economical indices. The simulation of microgrid in the Illinois Institute of Technology shows improvement reliability enhancement, namely through mitigation of interruption duration and frequency by the storage systems. Moreover, new indices have been used to describe reliability for the specific case of microgrids, as seen in [5].

The aforementioned studies assume the failure rate of the system's components to be constant, meaning that the probability that an element experiences a random fault is the same at all times, regardless of how the system is being operated. However, the current state of operation, *i.e.*, the system's current power flow, is expected to have an effect on the likelihood that one of its elements comes to a fault.

Xu *et al.* [6] propose a short term, hourly, reliability analysis, unlike the usual yearlong analysis carried out by utility companies. He also proposes the modeling of the system's failure rate as a function of its operating condition, and investigates its effect on both frequency and duration of interruptions. The probability of incorrect actions by the protection system is what is considered in this reference as responsible for the negative reliability impacts. However, [6] doesn't consider the effects on reliability caused by random failure, for example. This paper makes use of the concept of failure rate modeling, as well as the hourly dynamic analysis, but considers the voltages and currents resulting from power flow analysis to be the agent of failure rate change.

Voltage limits are set by ANSI regulations, while current limits are set by the manufacturers of each system component. This study considers faulted scenarios where these limits are not respected, to be faulted. The probability that the system's power flow is such that these limits are surpassed, is taken into consideration in this study and adds to the system's failure rate.

Once the reliability of the IEEE test system is quantified through a more traditional method of analysis [1], the proposed method of failure rate modeling is put into place for the same system, and results are compared. Given that an extra probability of failure is being considered for this second case, it is expected that the reliability indices will show a less reliable system. Given the local generation characteristic of a microgrid, the effect of DG sources regarding reliability is also investigated. A first scenario without DG sources is compared to a second scenario in which they are introduced. Finally, the impacts brought by storage systems are quantified. Because of the weather dependent power delivery behavior of renewables, storage systems are often adopted in microgrids.

The remainder of this paper is organized as follows: Section 2 discusses the mathematical modeling of both types of DG sources considered in this study (solar PV and wind), as well as the storage system. Also, the IEEE test system in which this basic analysis from [1] will be extended and applied is presented in this section. Section 3 presents the indices used to quantify reliability. Section 4 introduces the modeling of failure rate as a function of the resulting state variables from power flow. Section 5 brings the resulting indices for all studied scenarios. Section 6 draws conclusions and lays possible future improvements.

2. Microgrid Structure

2.1. Mathematical Modeling

The DG sources modeled in the microgrid, namely PV based and wind based are closely dependent of weather conditions, and are said to have intermittent output. Given that in this study, reliability analysis will be performed multiple times over a one year period, the changes in meteorological conditions will affect the power output of these DG sources and, as a consequence, the system's power flow.

Wind generators have power injection dependent on wind speed. Three velocity levels are designed by the manufacturer of a specific generator model: cut-in speed, nominal speed, and cut-out speed. For wind velocities of less than the nominal value, the generator's control will try to maximize the power absorbed from the wind by controlling the machine's torque. For cases with very low wind speeds, below cut-in value, the system is not able to convert any energy, and the power output is brought to zero. On the other hand, for wind velocities higher than nominal value, the angle between the generator's blades and the wind speed vector is adjusted by the

controller, such that the power delivered is constant and at nominal value, as well as minimizing mechanical stresses, assuring that there won't be any damages to the turbine. For cases with too high wind speeds, above cut-out speed, the controller will protect the blades and the power delivery will, again, be brought down to zero. This relationship is translated in Equation (1).

$$G_w = \begin{cases} G_{RATE} & V_{RATE} \le V < V_{co} \\ \dfrac{G_{RATE}\left(V - V_{ci}\right)}{V_{RATE} - V_{ci}} & V_{ci} \le V < V_{RATE} \\ 0 & \text{otherwise} \end{cases}. \quad (1)$$

G_{RATE} being nominal power given by the manufacturer. V_{ci}, V_{RATE}, and V_{co} are the cut-in wind speed, nominal wind speed, and cut-out nominal speed, respectively [6].

Two main factors that influence the performance of a solar cell include temperature and solar radiation. In [7], a 180 W ZED fabric mono-crystalline PV solar panel is tested, and the effects of varying operating temperature, as well as solar irradiation, are examined. It is seen that temperature has an impact more closely related to the cell's open circuit voltage, while irradiation has stronger impact on short circuit current. Regarding output power, the two factors have opposing effects: for higher temperatures, the cell's efficiency is reduced, while for higher values of irradiance, a better performance, with higher output power is obtained. This relation is modeled through Equations (2) and (3)

$$G_s = \frac{S}{S_{RATE}} \times \eta\left(E\right) \times G_{RATE}. \quad (2)$$

$$\eta\left(E\right) = 1 - 0.0045 \times \left(E - E_{RATE}\right). \quad (3)$$

where, E_{RATE} and S_{RATE} are the rated temperature of operation and rated solar radiation, in which the manufacturer determines the cell's parameters and performance.

Power and voltage supplied by a battery system have similar shape to what is shown in **Figure 1** [8]. Voltage drops from its maximum, charged value, to zero, following a curve that can be divided into three sections: first, the discharge section, in which it quickly drops from maximum to nominal value. Second, a section that can be seen, in practice, as linear and with constant voltage and power injected, as the battery discharges. Lastly, the exponential area, in which the State of Charge (SOC) of the battery exponentially drops to zero. In practice, operation is limited to the nominal section, meaning that the SOC is kept between 20% and 80% [9].

Given that this study is focused on reliability performance in steady state, a rather simple model of battery was adopted. Characteristics such as the influence of temperature, and internal resistances were disregarded. Also, the storage capacity drops along the life span of a battery. Typical battery systems have life spans of the order of thousands of cycles [10]. Since these systems are not expected to go through a full discharge cycle more than once a day, it is expected that this effect won't be relevant through the first year of the study. The operation strategy is set in such a manner as to discharge at a constant rate during the hours of peak load. The power injection was of 300 kW, and each system was capable of discharging over a period of 4 hours, with its SOC still remaining at the minimum of 20%. The system would be recharged back to an 80% SOC over the remaining hours

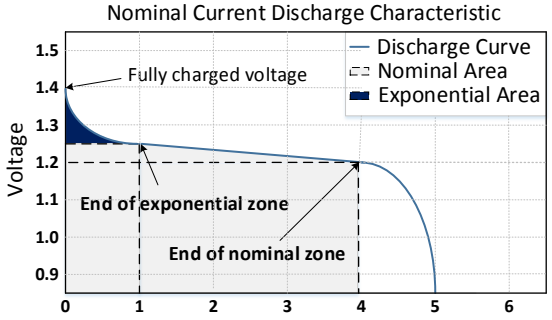

Figure 1. Battery discharge profile [8].

of lower load, which is done at a slower rate than the rate of discharge. The charging demand for the batteries was set to 100 kW.

2.2. Microgrid Test System

The test system adopted is presented in [11] focusing on the 11 kV system developed from BUS 4 of the RBTS. This distribution system is composed of 7 feeders connected in a loop through normally open tie-lines, connecting feeders F1 to F7, F3 to F4, as well as F5, F6 and F7 together. The total number of nodes and loadpoints are 67 and 38, respectively. All information necessary for reliability analysis is provided in [11]. The resulting indices for this system will be used for comparison with the results from this study.

The protection scheme for this system is as follows: all feeders are considered to have one main breaker on its head, connecting it to the main source. Lateral distributors are protected by fuses. Disconnectors are present, and are capable to isolate any faulted section in the main distributor. Finally, all loads beyond the faulted point are transferred through the tie-line to an alternative feeder, as long as the second feeder is capable to handle the extra load. In terms of failure rate, a constant value of 0.065 failures/yr·km on all feeders is adopted. The time of unavailability, or repair time, is of 0.5 hours for loads that are transferred between feeders, 5 hours for loads that are disconnected, and 200 hours for faults on a transformer.

Figure 2 shows the test system, and identifies the location in which the DG sources and the battery systems will be placed. Four utility scale DG sources are introduced, namely two PV systems of nominal power 2.0 and 2.5 MW, connected to nodes 62 and 38, respectively, and two wind based systems, with nominal power of 2.0 and 3.0 MW, connected to nodes 25 and 9, respectively. Two storage systems of nominal capacity 2 MWh each, are connected to nodes 44 and 50.

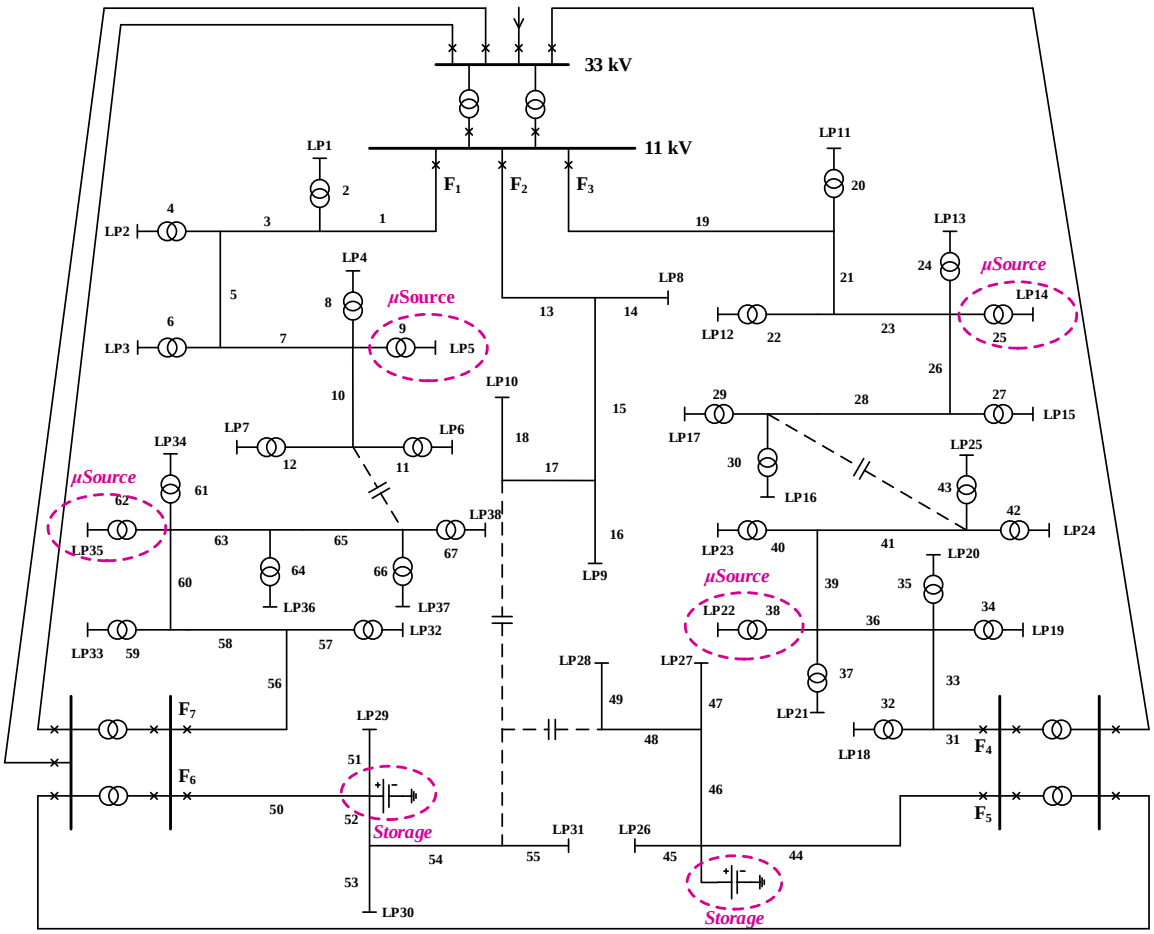

Figure 2. Microgrid test system with placement of DG sources and storage [11].

3. Reliability Quantification

Multiple different indices are used to quantify reliability. In this study, seven of them are being calculated, according to Equations (4) through (10): System Average Interruption Frequency (SAIFI), System Average Interruption Duration (SAIDI), Customer Average Interruption Duration (CAIDI), Average Service Availability (ASAI), Average Service Unavailability (ASUI), Energy Not Supplied (ENS) and Average Energy Not Supplied (AENS). Reference [1] goes in detail on reliability analysis, and how those indices are obtained.

$$SAIFI = \frac{\text{cust. interruptions}}{\text{cust. served}} = \frac{\sum \lambda_i N_i}{\sum N_i}. \tag{4}$$

$$SAIDI = \frac{\text{cust. interruption duration}}{\text{cust. served}} = \frac{\sum U_i N_i}{\sum N_i}. \tag{5}$$

$$CAIDI = \frac{\text{cust. interruption duration}}{\text{interruptions}} = \frac{\sum U_i N_i}{\sum \lambda_i N_i}. \tag{6}$$

$$ASAI = \frac{\text{available hours}}{\text{demanded hours}} = \frac{\sum 8760 N_i - \sum U_i N_i}{\sum 8760 N_i}. \tag{7}$$

$$ASUI = \frac{\text{unavailable hours}}{\text{demanded hours}} = 1 - ASAI. \tag{8}$$

$$ENS = \sum L_i U_i. \tag{9}$$

$$AENS = \frac{\text{energy not supplied}}{\text{cust. served}} = \frac{\sum L_i U_i}{\sum N_i}. \tag{10}$$

where, λ_i is the failure rate of ith element; U_i is the unavailability of ith element, given by the product of failure rate and outage time, N_i is the number of customers connected to loadpoint i L_i is the average load on loadpoint i.

4. A Heuristic Approach for Reliability Analysis

This section proposes a different approach on Failure Rate, considering it not only a simple constant, but a function of the current state of its distribution system, described by a power flow study. The resulting difference between this approach and the traditional reliability analysis will be evidenced in the next section, through the case study of the test system.

The power flow algorithm adopted was the Back/Forward Sweep Method, presented in [12]. This method showed to be simple, yet effective, and have good simulation time when compared to more traditional algorithms.

A reliability study is normally performed on nominal conditions of operation. However, in an actual distribution system, the conditions might not always be ideal, and components might be subjected to different values of voltage or current than what they were designed for. A component subjected to a stress beyond its nominal ratings is expected to have a higher probability of failure. Also, steady state voltage limits are established by the ANSI to be a minimum of 0.95 pu and a maximum of 1.05 pu [13]. As for currents, the maximum value that a component can withstand is determined by its manufacturer, and is called ampacity current. In transient operation, the same component can be subjected to even higher currents and still perform correctly, as long as the time of exposure is small enough. For both these reasons, the non-compliance of the system's currents or voltages to their maximum or minimum values is also regarded as a failure in this study.

State variables are a set of variables used to summarize the system's status. The state of a system, described by its state variables, is enough information to predict its future behavior, given that no external forces affect the system [14]. For the test system [11], its state variables are considered to be two: the set of system voltages, and the set of system currents. The state variables of the test system are, therefore, related to the probability of fail-

ure of its components.

Thus, a function between Failure Rate and state variables is proposed, working as a link between power flow analysis and reliability analysis. The state variables, resulting of power flow analysis, will serve as input to the modeling, which will result in an updated value of Failure Rate, serving as input to the reliability analysis. This way, a more realistic result on reliability is expected to be achieved.

The standard failure rate is, therefore, added of a new probability of failure, related to the noncompliance of the limits established by the norm. This is represented in Equation (11) [6].

$$\lambda_t(x) = \frac{P_t(x)}{\Delta t} + \lambda_o \times \frac{\Delta t}{8760}. \tag{11}$$

where, $\lambda_t(x)$ is the new failure rate, λ_o is the random failure rate of 0.065 failures/km·yr, and $P_t(x)$ is the additional probability of failure brought by the current state variables. Δt is the interval of time to be analyzed.

$P_t(x)$ is quantified by Equation (12), where the integral element gives the cumulative distribution function (CDF) of state variable x, from zero to x_s. For x being either current or voltage, x_s gives the short term rating value, indicating the feeder's capability in short term contingency operation [6]. The difference between the unity value and the CDF gives the probability that state variable x is beyond its acceptable short term maximum value, and, therefore, qualifies as a probability of failure. The term γ (gamma) gives the malfunctioning probability of the protection system, *i.e.* the probability that the protection elements operate facing no actual fault in the system, or that an actual fault occurs and the protection elements do not operate. That value is taken as a constant of 0.01

$$P_t(x) = 1 - \int_0^{x_s} f_t(x)\,\mathrm{d}x + \gamma. \tag{12}$$

It is assumed that state variable x follows a truncated normal distribution $f_t(x)$, with mean value x set. The sensitivity factor α is introduced to characterize the relationship between mean value $x$set and normal rating value x_n. Therefore, α is given by the ration between $x$set and x_n. With the mean value defined, a third parameter β is introduced to determine the amount of dispersion of the normal distribution, and is given by Equation (13), where δ is the variance of function $f(x)$. Parameter β is set to 5, while α is set to 1.3 for when state variable x represents current values, and 1.6 for when it represents voltage values

$$\beta = \frac{x_s - x_n}{\delta}. \tag{13}$$

Reliability analysis will be performed for each hour within a one year period, in this study. In each period Δt, $P_t(x)$ will be determined both for x being considered the system's currents and the system's voltages. The following reliability analysis will be performed for the worst case or, the highest of both modeled failure rates. The flowchart in **Figure 3** summarizes the analysis in this study.

5. Case Study

As shown in **Figure 3**, this study proposes a short term reliability analysis to be performed, such that the changes in the state of operation can be noticed and accounted for. The period of analysis is taken to be one hour. Thus, for every hour of a one year period, a new set of weather and load conditions will lead to new power flow results, which will affect the current state of failure rate, and the index values for that one hour period. At the end of the year, the final indices can be given as the sum of all indices (with exception of ASAI and ASUI which are taken as the average of all hourly indices).

Since [11] only provides constant values of load demand for the test system, a load demand profile had to be obtained. That information was taken from [15], whose measurements are taken from a residential area with peak demand of 10 MW (half the nominal demand of the test system). This hour by hour load profile was used to scale the maximum load demand on each loadpoint of the test system. The scaling coefficients are plotted in **Figure 4**.

Temperature and solar illuminance yearly profiles were obtained from measurements made by National Renewable Energy Laboratory, located in Oak Ridge, TN, throughout the year of 2014 [16]. For wind speed profile,

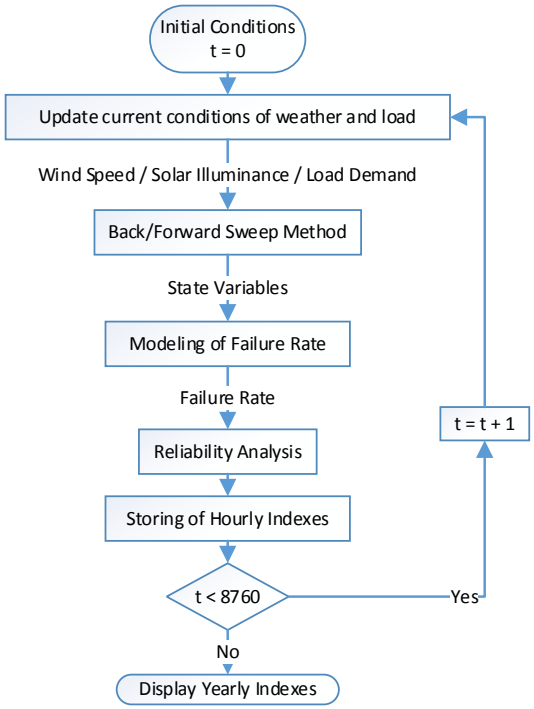

Figure 3. Flowchart of study.

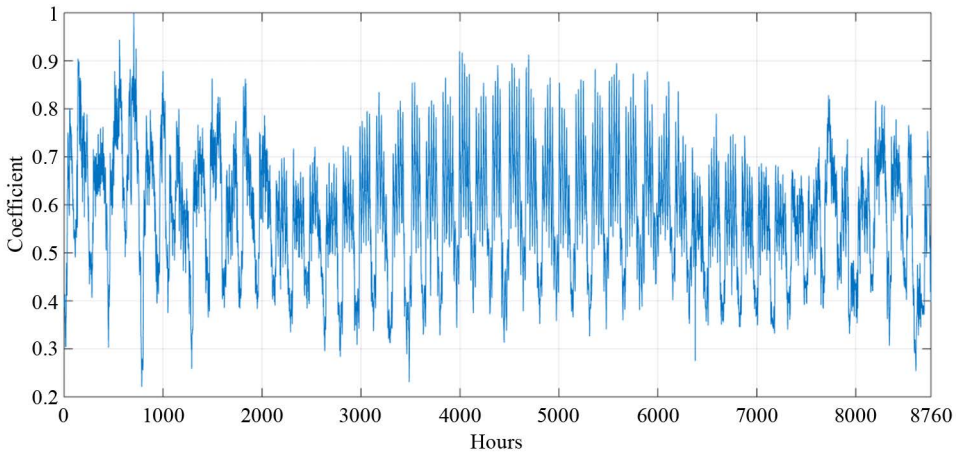

Figure 4. Yearly load demand profile.

the database of NASA's Modern-Era Retrospective Analysis for Research and Applications [17] was used. The information was related to the North Carolina area, more precisely to coordinates 34.5˚N/−83˚W, during the year of 2014. **Figure 5** shows a plot for both illuminance (yellow curve) and solar illuminance (blue curve) used. It is noticed that illuminance is stronger during the middle months of the year, while wind is stronger during earlier or later months.

Figure 6 through 12 shows the resulting indices for the hourly analysis of each of the 7 indices presented in section III. For each of those indices, both scenarios with and without DG sources are plotted, so that the effects of micro source power injection can be evidenced. Notice how the format of the indices for the scenarios with failure rate modeling follows a shape similar to the load profile, shown in **Figure 4**, given that it is the increase in load demand that results in higher currents and voltage drops and, therefore, higher probability of having inadequate state variables. Also, in each of the figures, a constant line shows the result obtained through basic reliability analysis, considering only standard failure rate λ_o.

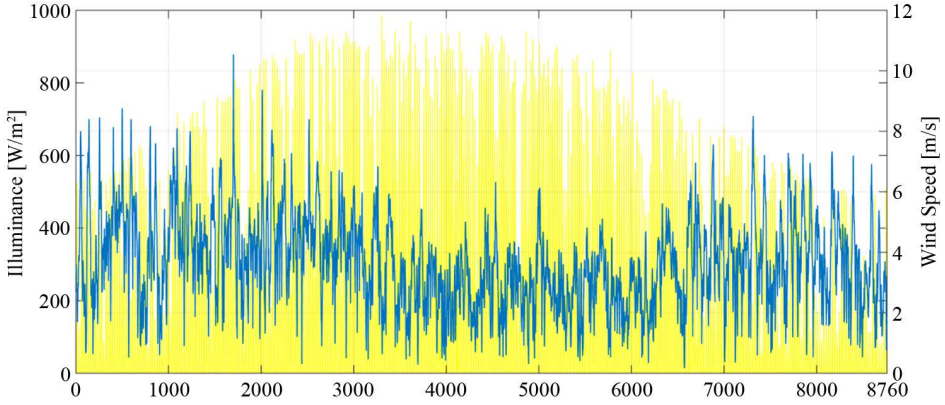

Figure 5. Yearly profile of solar illuminance and wind speed.

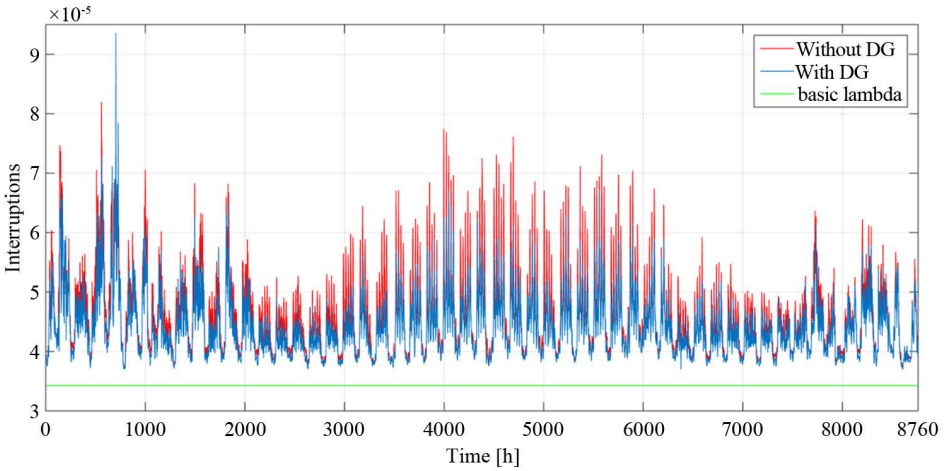

Figure 6. Hourly behavior ofthe SAIFI index over the one year study.

Figure 6 shows that SAIFI was increased (worsened) when compared to the basic failure rate results represented by the green horizontal line, due to the Failure Rate Modeling. Once the probability of having inadequate state variable values is taken into consideration as a fault probability, the failure rate of the system is increased and the resulting indices are generally worsened. For the case with DG, both indices are reduced (improved), when compared to the results without DG, and the reduction is more visible during the middle months of the year, when PV injection is at its highest. SAIDI shows similar behavior.

Figure 7 shows the results for CAIDI. For this index, as opposed all others, an improvement (reduction) is noticed when the state variables are considered into the failure rate modeling. This means that, on average, the interruptions in the system will have a shorter duration. This improvement is due to the fact that the increased failure rate is only considered for cable failure in the system. Other elements also have probability of failure, and for those, the outage time might be much larger, such as those of lateral transformers, whose outage time is of 200 hours.

ASAI is shown in **Figure 8** to be reduced (worsened), when compared to the basic failure rate case. This index translates the availability of the system. Due to the increase in failure rate, the system is expected to be less reliable and less available. Once DG injection is considered, this index is slightly improved. Naturally, ASUI has the exact opposite behavior, given that this index translates system unavailability.

Figure 9 shows ENS to have similar behavior to SAIFI and SAIDI, except the reduction in these two indices brought by the DG sources is more discrete. AENS, as being simply the average ENS index, shows similar profile.

Table 1 summarizes the indices for the first two scenarios, and compares it to the basic results as presented in [11] (reference). The new set of indices calculated using modeled failure rate are shown in the two middle

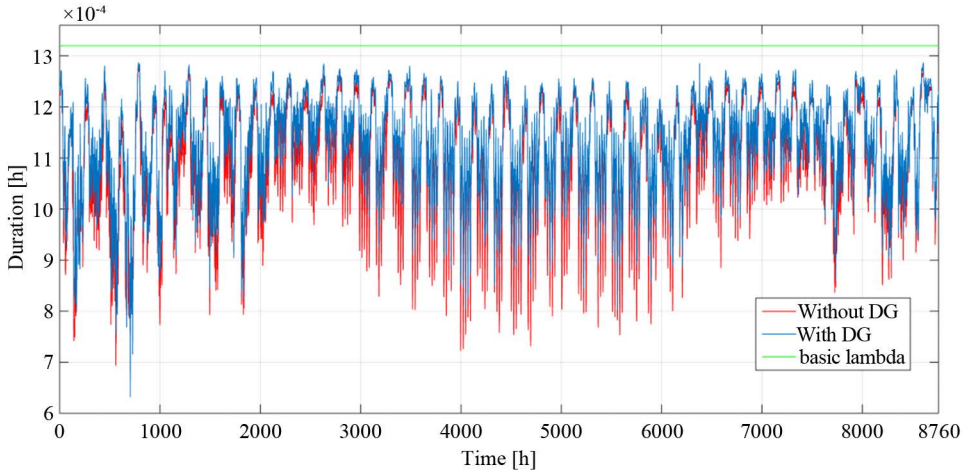

Figure 7. Hourly behavior of the CAIDI index over the one year study.

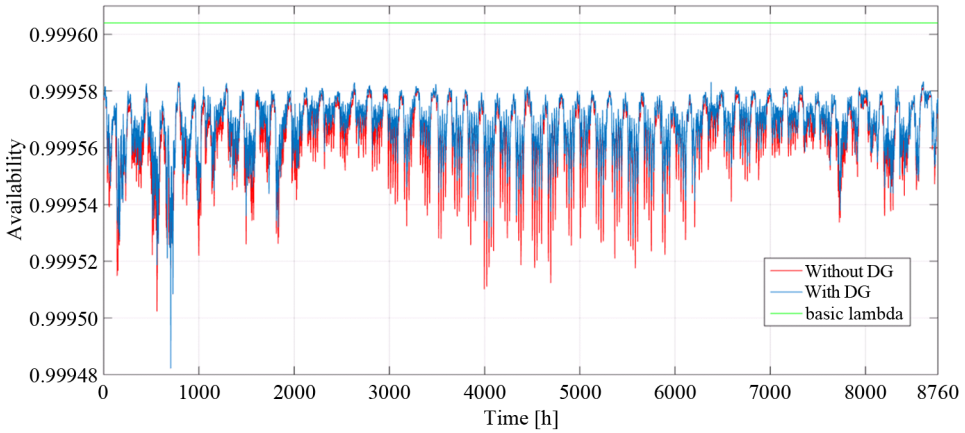

Figure 8. Hourly behavior of the ASAI index over the one year study.

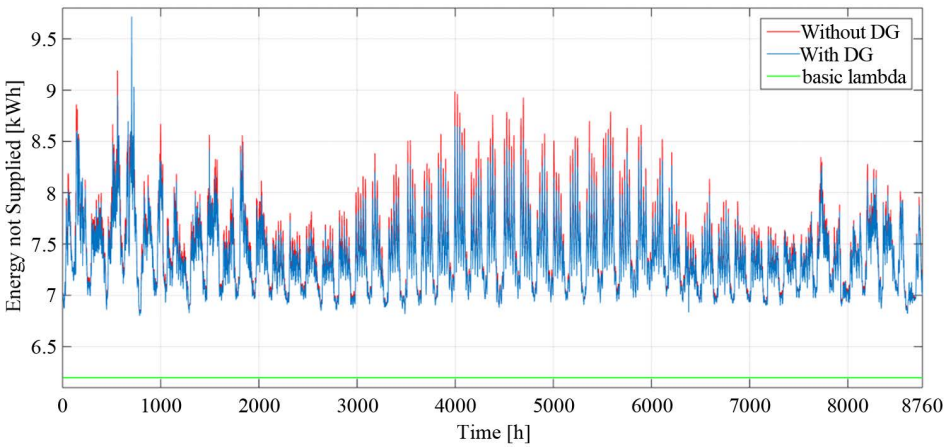

Figure 9. Hourly behavior of the SAIFI index over the one year study.

columns, and have their percentual impact indicated. The same is shown for the second scenario, in which the DG sources are introduced into the microgrid.

The initial assumption for the storage system was to connect them to two out of the same four LPs the DG sources were connected to. However, the reliability improvement was negligible. A new placement on nodes 44

Table 1. Resulting yearly indices for the two first scenarios: analysis with failure rate modeling, and analysis with failure rate modeling and insertion of DG sources. Traditional reliability analysis is used as reference.

	Reference	Failure Rate Modeling		With DG	
	Index	Index	Gain (%)	Index	Gain (%)
SAIFI	0.3	0.404	+34.67	0.385	−4.70
SAIDI	3.47	3.82	+10.09	3.78	−1.05
CAIDI	11.56	9.58	−17.13	9.90	+3.34
ASAI	0.999604	0.999564	−0.0040	0.999568	+0.0004
ASUI	3.96E−04	4.36E−04	+10.10	4.31E−04	−1.15
ENS	54293	65068	+19.85	64626	−0.68
AENS	11.36	13.62	+19.89	13.52	−0.73

Table 2. Resulting yearyl indices for the third scenario: introduction of storage systems. Comparison performed with second scenario.

Index	Without Storage	With Storage	Gain (%)
SAIFI (int/cus-yr)	0.385	0.379	−1.56
SAIDI (h/cus-yr)	3.78	3.63	−3.97
CAIDI (h/int)	9.90	9.66	−2.42
ASAI	0.999568	0.999585	+0.0017
ASUI	4.31E−04	4.14e−04	−3.94
ENS (MWh/yr)	64626	61568	−4.73
AENS (kWh/cus-yr)	13.52	12.88	−4.73

and 50 was proposed, as was shown in **Figure 2**. The impact brought by these systems is shown in **Table 2**, compared to the second scenario.

6. Conclusions

The consideration of noncompliance of system state variables to the probability of failure (failure rate) resulted in worsening of all indices to a smaller or larger degree, with the exception of the CAIDI. The average impact was of a worsening of 11.07%, meaning that the traditional method or obtaining elements' failure rates left certain factors out of the picture, which could result in considerable overestimations of system reliability. The introduction of DG sources within the microgrid and closer to the loads reduced the power flow intensity, mitigating the negative effects brought by the Failure Rate Modeling. However, this positive impact was rather small, having an average improvement of 0.71% over all seven indices, partially because the weather conditions were such that the DG sources operated below nominal power for most of the time. Also, given that the microgrid system was considered to be connected to an ideal infinity bus, the contribution of the DG sources was limited, for their larger impact would occur for faulted cases in the main grid, where the loads would be supplied only by the local generation. In those cases, the reliability indices would be deeply affected by the absence of DG sources. The last scenario aimed to investigate the impacts brought by storage systems, which would be responsible for balancing the irregular power injection profile of the DG sources caused by their weather dependent characteristics. These systems had an average contribution of 3.05% in the indices. Similar to the DG sources, the storage systems might have even higher impact if the possibility of fault in the main grid was being considered. For that case, a different logic of charge and discharge might need to be applied.

Valuable additions could be made to this study in the future: the failure rate modeling was only applied to cables and buses. The distribution transformers were also possible faulted elements, and might need to be considered. Second, a slightly more complete reliability analysis could be run, including the possibility of faults

outside the microgrid, to which the system would respond by disconnecting itself and operating in off-grid mode. This would reduce the overall reliability of the system, but would better evidence the impacts of both the storage system and the DG sources. Lastly an optimal placement algorithm might be applied for the storage systems.

References

[1] Billinton, R. and Allan, R. (1996) Reliability Evaluation of Power Systems. 2nd Edition, Springer, Chichester, 514 p.

[2] Bae, I.S. and Kim, J.O. (2007) Reliability Evaluation of Distributed Generation Based on Operation Mode. *IEEE Transactions on Power Systems*, **22**, 785-790. http://dx.doi.org/10.1109/TPWRS.2007.894842

[3] Bae, I.S. and Kim, J.O. (2008) Reliability Evaluation of Customers in a Microgrid. *IEEE Transactions on Power Systems*, **23**, 1416-1422.

[4] Khodayar, M.E., Barati, M. and Shahidehpour, M. (2012) Integration of High Reliability Distribution System in Microgrid Operation. *IEEE Transactions on Smart Grid*, **3**, 1997-2006. http://dx.doi.org/10.1109/TSG.2012.2213348

[5] Wang, S., Li, Z., Wu, L., Shahidehpour, M. and Li, Z. (2013) New Metrics for Assessing the Reliability and Economics of Microgrids in Distribution System. *IEEE Transactions on Power Systems*, **28**, 2852-2861. http://dx.doi.org/10.1109/TPWRS.2013.2249539

[6] Xu, X., Mitra, J., Wang, T. and Mu, L. (2014) Evaluation of Operational Reliability of a Microgrid Using a Short-Term Outage Model. *IEEE Transactions on Power Systems*, **29**, 2238-2247. http://dx.doi.org/10.1109/TPWRS.2014.2303792

[7] Nayan, M.F. and Ullah, S.M.S. (2015) Modelling of Solar Cell Characteristics Considering the Effect of Electrical and Environmental Parameters. 3*rd International Conference on Green Energy and Technology* (*ICGET*), Dhaka, 11 September 2015, 1558-6261. http://dx.doi.org/10.1109/icget.2015.7315096

[8] Tremblay, O., Dessaint, L.-A. and Dekkiche, A.-I.(2007) A Generic Battery Model for the Dynamic Simulation of Hybrid Electric Vehicles. *Vehicle Power and Propulsion Conference*, Arlington, 9-12 September 2007, 1004-4454. http://dx.doi.org/10.1109/vppc.2007.4544139

[9] Chahwan, J.A. (2007) Vanadium-Redox Flow and Lithium-Ion Battery Modelling and Performance in Wind Energy Applications. M. Eng. Thesis, McGill University, Montreal.

[10] Akhil, A.A., *et al.* (2013) DOE/EPRI 2013 Electricity Storage Handbook in Collaboration with NRECA. http://www.sandia.gov/ess/publications/SAND2013-5131.pdf

[11] Allan, R.N., Billinton, R., Sjarief, I., Goel, L. and So, K.S. (1991) A Reliability Test System for Educational Purposes-Basic Distribution-System Data and Results. *IEEE Transactions on Power Systems*, **6**, 813-820. http://dx.doi.org/10.1109/59.76730

[12] Ghosh, S. and Das, D. (1999) Method for Load-Flow Solution of Radial Distribution Networks. *IEE Proceedings-Generation, Transmission and Distribution* (1999), **146**, 641. http://dx.doi.org/10.1049/ip-gtd:19990464

[13] National Electrical Manufacturers Association (2005) Electric Power Systems and Equipment-Voltage Ratings (60 Hertz). American National Standards Institute, Inc. ANSI C.84-1-1995, Virginia, 26 p.

[14] Brogan, W.L. (1990) Modern Control Theory. 3rd Edition, Pearson.

[15] Duke Energy (2014) Duke Energy SCADA Historian. http://www.duke-energy.com/pdfs/dmainitiative.pdf

[16] National Renewable Energy Laboratory (2016) Daily Plots and Raw Data Files.

[17] NASA (2015) MERRA: Modern-Era Retrospective Analysis for Research and Applications. http://gmao.gsfc.nasa.gov/research/merra/